

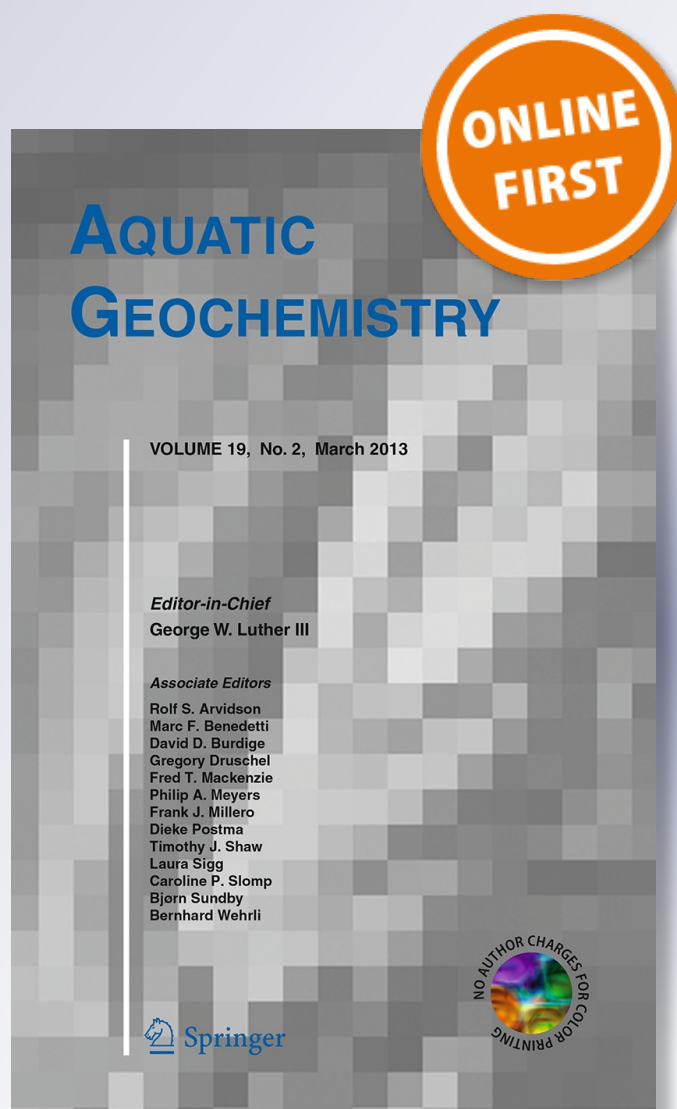
*Rates of Biotite Weathering, and
Clay Mineral Transformation and
Neoformation, Determined from
Watershed Geochemical Mass-Balance
Methods for the Coweeta Hydrologic
Laboratory, Southern Blue Ridge
Mountains, North Carolina, USA*
Jason R. Price & Michael A. Velbel

Aquatic Geochemistry

ISSN 1380-6165

Aquat Geochem

DOI 10.1007/s10498-013-9190-y



Your article is protected by copyright and all rights are held exclusively by Springer Science +Business Media Dordrecht. This e-offprint is for personal use only and shall not be self-archived in electronic repositories. If you wish to self-archive your work, please use the accepted author's version for posting to your own website or your institution's repository. You may further deposit the accepted author's version on a funder's repository at a funder's request, provided it is not made publicly available until 12 months after publication.

Rates of Biotite Weathering, and Clay Mineral Transformation and Neof ormation, Determined from Watershed Geochemical Mass-Balance Methods for the Coweeta Hydrologic Laboratory, Southern Blue Ridge Mountains, North Carolina, USA

Jason R. Price · Michael A. Velbel

Received: 15 October 2012 / Accepted: 1 March 2013
© Springer Science+Business Media Dordrecht 2013

Abstract Biotite is a common constituent of silicate bedrock. Its weathering releases plant nutrients and consumes atmospheric CO₂. Because of its stoichiometric relationship with its transformational weathering product and sensitivity to botanical activity, calculating biotite weathering rates using watershed mass-balance methods has proven challenging. At Coweeta Hydrologic Laboratory the coupling of biotite to its transformational weathering product is only valid if the stoichiometric relationship for the two phases is known; this relationship is unlikely layer-for-layer. Rates of biotite weathering and transformation of its secondary weathering product at the Coweeta Hydrological Laboratory are comparable with other Appalachian watersheds. The magnitude and sign of the difference between field- and laboratory-determined biotite weathering rates are similar to those of other silicate minerals. The influence of major-cation proportions in biomass on the rates of biotite weathering and transformational weathering product is greatest for watersheds with high biomass aggradation rates. The watershed with the lowest bedrock reactivity and highest flushing rate yielded the highest gibbsite formation rate of ~500 mol ha⁻¹ year⁻¹ and lowest kaolin-group mineral formation rates of 4–78 mol ha⁻¹ year⁻¹. The kaolin-group mineral formation rate increases as bedrock reactivity increases and flushing rate decreases to a maximum of ~300 mol ha⁻¹ year⁻¹, with a similar minimum gibbsite formation rate. The relative differences in bedrock reactivity and flux of water through Coweeta Hydrological Laboratory watersheds studied appear to be invariant over geologic timescales.

Keywords Biotite · Weathering · Watersheds · Mass balance · Rates · Clays

J. R. Price (✉)

Department of Earth Sciences, Millersville University, P.O. Box 1002, Millersville,
PA 17551-0302, USA
e-mail: Jason.Price@millersville.edu

M. A. Velbel

Department of Geological Sciences, Michigan State University, 288 Farm Lane,
206 Natural Science Building, East Lansing, MI 48824-1115, USA

1 Introduction

The ability to accurately quantify mineral weathering is essential for studies of ecosystems, global geochemical cycles including the carbon cycle, and climate change (e.g., Likens and Bormann 1995; Berner and Berner 1997; Gaillardet et al. 1999). Small-watershed solute mass-balance methods are commonly used for identifying weathering reactions in natural systems (Bricker et al. 2003). Characterizing minerals that weather by simple stoichiometric dissolution may be relatively simple in mass-balance studies. However, other minerals such as the micas weather to secondary products by complex crystal-chemical transformations. Because biotite mica contains appreciable quantities of the plant nutrients Mg^{2+} and K^+ , calculation of its weathering rate may be further complicated if the biomass is actively aggrading or degrading, and/or the nutrient uptake stoichiometry is not accurate. Therefore, the calculation of biotite weathering rates, including the rates of formation of biotite's transformational weathering products, using watershed mass-balance methods has proven to be very challenging and has never been systematically investigated.

This paper examines natural field-based biotite weathering rates in a series of case studies inspired by the pioneering work of Owen Bricker and his colleagues. Over the course of his productive career, Owen Bricker has studied the kinetics of biotite weathering both experimentally (i.e., Acker and Bricker 1992) and in small-watershed mass-balance studies of reaction stoichiometries (e.g., Cleaves et al. 1970; O'Brien et al. 1997). This paper examines Bricker's views on the mechanism and stoichiometry of biotite weathering reactions, and nature and rates of formation of secondary weathering products used in small-watershed solute studies. Several of these approaches were invoked in successive iterations of research by Velbel and his students in their research at the Coweeta Hydrologic Laboratory (CHL) (Velbel 1985a, b, 1986, 1988, 1995; Taylor and Velbel 1991; Price et al. 2005a; Velbel and Price 2007).

2 Background

2.1 Biotite

Mica weathering is the dominant natural source of K^+ to terrestrial ecosystems (e.g., Fanning and Keramidas 1977; Thomsson and Ukrainczyk 2002) and is capable of affecting the mobility of certain contaminant species in and through soils (e.g., Smith et al. 1999; Thomsson and Ukrainczyk 2002). Consequently, mica weathering has long been a topic of special interest to soil scientists, and much of the research on mica weathering is found in the soil science literature rather than in the geochemical literature. Micas are a major constituent of granitic bedrock, with granitic rocks constituting $\sim 25\%$ of the land surface of the mean upper crust (Oliva et al. 2003). In addition, weathering of granitic bedrock is responsible for 65–70% of the global flux of CO_2 consumption derived from continental silicate weathering (Dessert et al. 2003). This discussion is confined to the weathering of naturally occurring biotite, because it is one of the most abundant, most weatherable, and best studied micas.

Micas are phyllo- (layer) silicate minerals that contain tightly held interlayer cations that balance the high layer charge (Fanning and Keramidas 1977). The ideal mica structure consists of two tetrahedral (*T*) sheets and one octahedral (*O*) gibbsite- or brucite-like sheet, in the *T:O* = 2:1 (*T–O–T*) “sandwich” structure. It is customary to deal with mica's stoichiometry in terms of the half unit-cell with the anion basis of $O_{10}(OH)_2^{2-}$ formula

unit. As in all common silicate minerals, tetrahedral sites are occupied by Si^{4+} and Al^{3+} . The substitution of Al^{3+} for Si^{4+} in one-fourth of the tetrahedral sites in micas gives rise to a deficiency of positive charge within the 2:1 layer in the amount of one charge per half unit-cell. This positive layer-charge deficiency is balanced by occupancy of the interlayer cation site, typically K^+ .

In biotite, all octahedral sites are occupied, usually with Fe^{2+} or Mg^{2+} , and thus, biotite is termed trioctahedral, in contrast to dioctahedral micas which have two out of every three octahedral sites occupied, usually by Al^{3+} . Biotite is the name for a complete solid solution series of the trioctahedral end members annite ($\text{KFe}_3(\text{Si}_3\text{Al})\text{O}_{10}(\text{OH})_2$), phlogopite ($\text{KMg}_3(\text{Si}_3\text{Al})\text{O}_{10}(\text{OH})_2$), siderophyllite ($\text{K}_2(\text{Fe}_5\text{Al})(\text{Si}_5\text{Al}_3)\text{O}_{20}(\text{OH})_4$), and eastonite ($\text{K}_2(\text{Mg}_5\text{Al})(\text{Si}_5\text{Al}_3)\text{O}_{20}(\text{OH})_4$). Biotite is common and widespread through a variety of geologic environments (Deer et al. 1966).

2.2 Compositional Changes During Biotite Weathering

Results of numerous chemical analyses of weathered biotite (including electron probe microanalyses, for example, Meunier and Velde 1979a) have suggested that mica weathers to vermiculite by way of a “simple transformation” (Fanning and Keramidas 1977). This transformation is dominated by exchange of interlayer potassium for hydrated exchangeable cations and possibly non-exchangeable hydrated Al^{3+} , which gives rise to the fixed 14 Å spacing of “pedogenic chlorite.” This interlayer exchange is often accompanied by changes in layer charge (Norrish 1973) due in part to oxidation of octahedral Fe^{2+} and to possible gains and losses of other octahedral cations (e.g., Newman and Brown 1966; Gilkes et al. 1972). Fanning and Keramidas (1977) suggested that this type of reaction be termed a “simple transformation” because a considerable portion of the mica 2:1 layer is retained in the weathering product. The definitive treatment of this phenomenon by electron microscopy is that of Banfield and Eggleton (1988).

2.3 Determining Biotite Weathering Rates in Nature by Watershed Solute Mass Balance

Determining rates of natural weathering of silicate minerals by solute mass balance began with the input–output budgeting “balance sheet” approach of Garrels and Mackenzie (1967). In this approach, the solute chemistry of a natural water attributable to mineral weathering is determined by sequentially subtracting quantities of dissolved products in proportions determined by stoichiometries of mineral weathering reactions. Subtractions of the mineral weathering contributions continue until only the solute abundances from atmospheric precipitation remain. Garrels and Mackenzie (1967) explained the compositions of Sierra Nevada spring waters as the consequence of the weathering of plagioclase feldspar, potassium feldspar, and biotite (using phlogopite as a simplified proxy) to clay minerals. For the case of deep circulation of water, smectite was invoked as a weathering product of plagioclase. For all primary minerals in the case of shallow circulation, the weathering product was kaolinite.

Very soon after the work of Garrels and Mackenzie (1967), Bricker et al. (1968) performed a similar exercise on data from the Pond Branch watershed in Maryland, invoking a similar ensemble of weathering reactions. In contrast to relying solely on solute concentrations as did Garrels and Mackenzie (1967), Bricker et al. (1968) combined precipitation, stream discharge, and stream-chemistry data to yield input–output budgets applicable at the watershed scale (Cleaves et al. 1970; Puckett and Bricker 1992). This

allowed for calculation of elemental fluxes from the watershed and thereby introduced time and rates into watershed solute mass balance. The silicate weathering reactions invoked by Bricker et al. (1968) included weathering of plagioclase feldspar to kaolinite and gibbsite, and weathering of biotite to kaolinite. Cleaves et al. (1970) expanded the interpretation of solute production by silicate weathering at Pond Branch by using additional hydrologic and geochemical measurements. After a largely quiet decade, emerging concerns about landscape and surface-water acidification by acid deposition stimulated a torrent of papers beginning in the 1980s using solute-flux-based watershed mass balance to quantify natural surface-water processes, including mineral weathering rates (e.g., reviews by Bricker et al. 2003; White 2003; Velbel and Price 2007, and primary references therein).

Following widely held views about structurally controlled mica weathering (summarized by Gilkes and Suddhiprakarn 1979a), Cleaves et al. (1970) invoked separate weathering reactions for biotite weathering to vermiculite and subsequent vermiculite weathering to kaolinite. In the biotite–vermiculite reaction of Cleaves et al. (1970), three $O_{20}(OH)_4$ units of biotite weathered to two $O_{20}(OH)_4$ units of vermiculite. In the vermiculite–kaolinite reaction, further weathering of two $O_{20}(OH)_4$ units of vermiculite produced three $O_5(OH)_4$ units of kaolinite. In their comparative study of five Mid-Atlantic watersheds with diverse parent lithologies, O'Brien et al. (1997) document both vermiculite and kaolinite as weathering products. Their mass-balance model results yield much smaller amounts of vermiculite formed than biotite weathered.

Early linear-/matrix-algebra solutions to systems of simultaneous small-watershed solute mass-balance equations often needed to reduce the number of unknowns (mineral weathering rates) in order to equal the number of (mass balance) equations that could be written for elements with measured solute fluxes (Velbel 1985a, 1986; Taylor and Velbel 1991; Velbel and Price 2007). One approach was to write a weathering reaction by linking the production rate of a weathering product to the destruction rate of a specific reactant mineral. Velbel and Price (2007) used the term “coupling” to refer to calculating the formation rate of a specific clay mineral from that clay’s stoichiometric relationship with the weathering rate of a primary mineral. For the case of simple, direct transformational layer-by-layer replacement of biotite by vermiculite (e.g., Fanning and Keramidas 1977; Banfield and Eggleton 1988), for each mole of biotite weathered, one mole of vermiculite forms. This approach reduces the number of unknowns in watershed mass-balance calculations by one while retaining the same number of mass-balance equations. This approach was used in early weathering studies at CHL (Velbel 1985a, 1986; Taylor and Velbel 1991). Other coupled biotite–vermiculite relationships have also been invoked. For example, as noted above, three $O_{20}(OH)_4$ units of biotite weather to two $O_{20}(OH)_4$ units of vermiculite in reaction (4) of Cleaves et al. (1970). Banfield and Eggleton (1988) reported some evidence of transformation of two biotite layers to one vermiculite layer. For the Loch Vale watershed, Colorado, Mast et al. (1990) and Mast (1992) invoked 0.87 mol of smectite–illite forming for every mole of biotite weathered. In contrast, vermiculite production was decoupled from biotite-layer destruction in the approach used by O'Brien et al. (1997) and later at CHL by Price et al. (2005a). Transmission electron microscopic evidence for the decoupling of biotite from its kaolinitic weathering product(s) has been reported by Banfield and Eggleton (1988), Murphy et al. (1998), and Dong et al. (1998).

Inspired by the pioneering work of Owen Bricker and his colleagues, this paper examines the influence of stoichiometric coupling of the biotite weathering rate and the formation rate of its transformation weathering product at the Coweeta Hydrologic Laboratory. The influence of diverse assumptions about stoichiometric coupling on weathering rates determined by watershed solute mass balance during the past several decades is investigated.

2.4 Study Site

The Coweeta Hydrologic Laboratory is located in the southeastern Blue Ridge Physiographic Province of western North Carolina (Fig. 1). The CHL watersheds are well suited for studies of chemical weathering as they are geomorphically intermediate between transport- and weathering-limited regimes (Stallard and Edmond 1983). The Coweeta Basin is quite rugged (average slope of approximately 45 %/23°) and is underlain by the amphibolite facies metasediments of the mid-Ordovician Coweeta Group (Hatcher 1988; Miller et al. 2000) and the Upper Precambrian Otto Formation (Hatcher 1980, 1988). The Coweeta Group is composed of a massive quartz diorite orthogneiss, quartz-feldspar gneisses, pelitic schists, quartzites, and metasandstones, reflecting protoliths consisting of relatively mature sediments, including arkoses and quartz arenites (Hatcher 1980). The Otto Formation is derived from sedimentary protoliths of low compositional maturity (e.g., graywackes) and is predominantly biotite paragneiss and biotite schist (Hatcher 1980). The greater abundance of biotite and plagioclase in the Otto Formation makes it significantly more chemically reactive than the more quartz-rich Coweeta Group. Coweeta Group and Otto Formation rocks are juxtaposed as a result of thrusting of the premetamorphic Shope Fork Fault (Hatcher 1988; Fig. 1). Specific characteristics of each watershed investigated are reported in Table 1.

Saprolite mantles the landscape at CHL, although bedrock crops out locally, especially near ridge crests. The average weathering profile (saprolite and soil) at CHL is

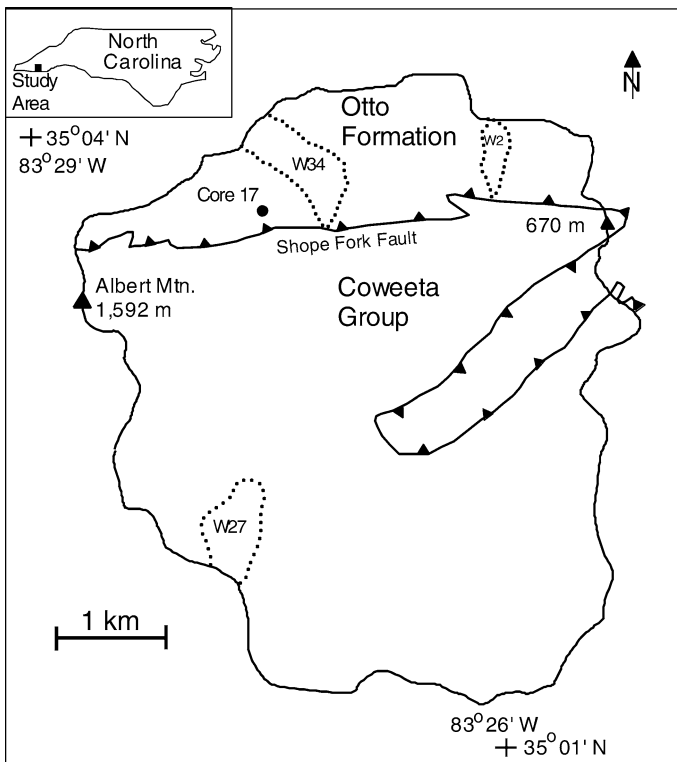


Fig. 1 Map of Coweeta Hydrologic Laboratory showing control watersheds investigated in this study, the location of Core 17, and bedrock geology

Table 1 Characteristics of the control watersheds of Coweeta Hydrologic Laboratory investigated in this study, with data from Swank and Crossley (1988), Swank and Waide (1988), and Swift et al. (1988)

Watershed	Bedrock	Area (ha)	Precipitation (cm year ⁻¹)	Mean elevation (m)	Temperature (°C)	Discharge (m ³ ha ⁻¹ day ⁻¹)	SiO ₂ Flux (mol ha ⁻¹ year ⁻¹)
2	Otto Formation	12	177	857	11.7	25	1,277
34	Otto Formation	33	201	1,025	10.6	35	1,321
27	Coweeta Group	39	245	1,258	9.1	51	1,083

approximately 6 m thick (Berry 1976; Yeakley et al. 1998), with a maximum thickness of 18 m (Berry 1976; Ciampone 1995). Soils (mostly Ultisols and Inceptisols) constitute the uppermost 30 cm of the profile (Velbel 1985a, 1988). The minerals involved in weathering at CHL are allanite, plagioclase feldspar, garnet, biotite, vermiculite, kaolinite, and gibbsite (Velbel 1985a; Taylor and Velbel 1991; Price et al. 2005a). An extensive ground water aquifer has not been shown to exist at CHL (Hewlett 1961). Instead, nearly all stream water passes through the soil and saprolite mantle, with continuous base flow to perennial streams resulting from water draining from pore space in the unsaturated zone (Hewlett 1961; Hewlett and Hibbert 1963; Velbel 1985b). Velbel (1985b) demonstrated that the streams at CHL are samples of subsurface water which have undergone no significant change after leaving the saprolite to enter the streams, except re-equilibration with atmospheric gases which affect pH.

3 Methods

3.1 Petrography

Thin sections of bedrock were prepared following standard methods. Friable soil and saprolite were impregnated with epoxy prior to thin sectioning. Regolith was often sampled using a chrome tube to preserve the fabric of the material. Material within the tube was impregnated with epoxy prior to removal for thin section preparation.

3.2 Electron Microprobe Analyses (EMPA)

Electron microprobe analyses of bedrock biotite and regolith fresh and weathered biotite in thin section were completed at the University of Michigan's Electron Microbeam Analysis Laboratory (EMAL), using a wavelength dispersive Cameca SX 100 electron microprobe analyzer. Accelerating voltage and beam current were 15 keV and 10 nA, respectively, and a 2 µm beam diameter. Calculation of the stoichiometric formula for primary minerals from the EMPA data followed conventional methods. The stoichiometric formulae of the biotite weathering products were calculated using a method that assumes that the aluminosilicate layers have not been altered during the transformation of biotite to vermiculite (Newman 1987; Velbel 1984a, 1985a).

3.3 X-Ray Diffractometry (XRD)

Separation into the clay-size fraction was performed by gravity settling, with the clay-size fraction being separated with a pipette, and the aliquots being filtered onto a 0.45 µm

Millipore™ filter following rapid-suction mounting techniques (production of oriented mounts; also termed the Millipore™ Filter Transfer Method of Drever 1973). This method is well described by Moore and Reynolds (1997). In order to ensure homogeneity of the clay cakes on the filter, the clay solution was stirred during suction. The filter cake was transferred to standard petrographic slides without rolling after inverting onto the glass slide (Moore and Reynolds 1997). Rolling the filter may cause segregations of clay minerals in the cake, disrupting the homogeneity.

The most effective method of identifying and characterizing the minerals of weathering profiles is X-ray diffraction (Hughes et al. 1994). The XRD used belonged to the Department of Geological Sciences at Michigan State University and was a Rigaku Geigerflex that used CuK α radiation. A nickel foil filter was used to ensure monochromatic radiation and low background count. Analyses were conducted on samples collected at all levels in the weathering profile (including bedrock), using divergence, receiving, and anti-scatters slits of 1/2°, 0.3 mm, and 2°, respectively, a step size of 0.02° 2 θ , and count times of 20 s.

Identification of diffractogram peaks followed Brown and Brindley (1984), Wilson (1987), Eslinger and Pevear (1988), and Moore and Reynolds (1997). The 10 Å peaks on XRD patterns are herein referred to as “mica,” because both biotite and muscovite are present in the CHL bedrock. No baseline correction was applied to diffractograms.

3.4 Scanning Electron Microscopy Secondary (SEM) and Backscattered Electron Imaging (BSE)

Polished and carbon or gold-coated thin sections, and SEM stubs of CHL bedrock and regolith were prepared for examination by SEM and analyzed by energy dispersive X-ray spectroscopy (EDS) for element composition. Imaging and analyses were performed at Michigan State University's Center for Advanced Microscopy (CAM) using a JEOL JSM-35CF SEM with EDS and BSE capabilities.

3.5 Biotite Weathering Reactions and Rates from Watershed Mass Balance

Calculation of mineral weathering rates by watershed mass-balance methods has been adapted from Plummer and Back (1980) and formally presented by Velbel (1986). For a system assumed to be in steady-state:

$$\sum_{j=1}^{\varphi} \alpha_j \beta_{c,j} = \Delta m_c \quad c = 1, \dots, n$$

Where, φ = number of unknowns; the number of transforming phases j ; α = the transformation rate of phase j [units of a flux (mol ha⁻¹ year⁻¹)]; β = the stoichiometric coefficient of species c in phase j ; Δm_c = the total change in mass of species c [units of a flux (mol ha⁻¹ year⁻¹)]; n = number of mass-balance equations.

The solution of n equations in $\varphi = n$ unknowns is mathematically unique, regardless of the stoichiometric coefficients used, and/or whether some additional process in addition to those described by the stoichiometric coefficients have been ignored (Taylor and Velbel 1991). The elemental flux out of a watershed is calculated by multiplying stream discharge by the elemental concentration of the stream water and dividing by watershed area (e.g., Creasey et al. 1986; Velbel 1985a, b); elemental flux into a watershed is similarly calculated from precipitation amounts and its chemical composition (Swift et al. 1988).

Balanced biotite weathering reactions that invoke coupling with its weathering product assume complete conservation of the biotite silicate sheet in the weathering product. By doing so, there is no gain or loss of Si^{4+} during weathering, but it may require import of Al^{3+} when a hydroxy-interlayer forms. When biotite weathering is decoupled from formation of its weathering product, there may be loss of both Al^{3+} and Si^{4+} as both the silicate sheet and the interlayer region may dissolve.

The coupling of biotite and its weathering product at CHL was used by Velbel (1985a) and Taylor and Velbel (1991). In such a scenario, the stoichiometric coefficients (β) for a given species c for biotite weathering becomes the difference between its stoichiometry in the biotite and its weathering product (Table 2). When biotite and its weathering product are coupled, the seven unknowns in the mass-balance calculations are the weathering or formation rates of allanite, plagioclase, garnet, biotite, kaolin-group minerals, gibbsite, and biomass. The term “kaolin-group minerals” is used herein to denote any clay mineral with the formula $\text{Al}_2\text{Si}_2\text{O}_5(\text{OH})_4$, which could be either kaolinite or halloysite. Such terminology is also consistent with recent chemical weathering work in the region (i.e., Schroeder et al. 2000; Velbel et al. 2009). For the seven unknown mineral weathering rates, the stream fluxes for SiO_2 , Al^{3+} , Mg^{2+} , Ca^{2+} , K^+ , Na^+ , and La^{3+} were used (after Price et al. 2005a). The eight weathering rates determined for the decoupled scenario (the same seven as in the coupled scenario, with the addition of vermiculite production) use flux values for the same seven elements as in the coupled scenario, but also included Dy^{3+} for Watersheds 2 and 34, and Nd^{3+} for Watershed 27 (after Price et al. 2005a). Price et al. (2005a, b) provide a detailed justification for the inclusion of rare earth elements (REE) in mass-balance calculations of CHL mineral weathering rates. Rare earth elements have been reported to fractionate between the solid- and solute-phases in streams (e.g., Ingri et al. 2000; Aubert et al. 2001; Gammons et al. 2005). However, sensitivity analyses indicate that the specific REE flux exerts relatively little influence on the calculated CHL mineral

Table 2 Chemical formulae for biotite and its weathering product at Coweeta Hydrologic Laboratory, North Carolina (modified from Price et al. 2005a)

Location	Phase	Structural/stoichiometric formula
Watersheds 2 and 34	Biotite	$\text{K}_{0.88}\text{Na}_{0.041}\text{Ca}_{0.001}$ $(\text{Mg}_{1.42}\text{Fe}_{1.05}\text{Mn}_{0.01}\text{Al}_{0.32}\text{Ti}_{0.097})(\text{Al}_{1.25}\text{Si}_{2.75})\text{O}_{10}(\text{OH})_2$
	Biotite Weathering Product of hydroxy-interlayered smectite (HIS)	$\text{K}_{0.48}\text{Na}_{0.032}\text{Ca}_{0.026}\text{La}_{0.000506}\text{Dy}_{0.0000734}(\text{Mg}_{1.54}$ $\text{Fe}_{0.27}^{\text{II}}\text{Fe}_{0.55}^{\text{III}}\text{Mn}_{0.005}\text{Al}_{0.33}\text{Ti}_{0.07})(\text{Al}_{1.25}\text{Si}_{2.75})\text{O}_{10}$ $(\text{OH})_2 \cdot 0.04\text{Al}_6(\text{OH})_{15}$
	Stoichiometric difference between biotite and its weathering product reflecting conservation of the silicate sheet (coupling)	$\text{K}_{0.40}\text{Mg}_{-0.12}\text{Ca}_{-0.025}\text{Na}_{0.009}\text{Al}_{-0.25}\text{La}_{-0.000506}$
Watershed 27	Biotite	$\text{K}_{0.91}\text{Na}_{0.028}$ $(\text{Mg}_{1.31}\text{Fe}_{1.16}\text{Al}_{0.33}\text{Ti}_{0.093})(\text{Al}_{1.25}\text{Si}_{2.75})\text{O}_{10}(\text{OH})_2$
	Biotite weathering product of hydroxy-interlayered smectite (HIS)	$\text{K}_{0.13}\text{Na}_{0.030}\text{Ca}_{0.017}\text{Mg}_{0.17}\text{La}_{0.000286}\text{Nd}_{0.000359}$ $(\text{Mg}_{0.80}\text{Fe}_{0.55}^{\text{II}}\text{Fe}_{0.79}^{\text{III}}\text{Mn}_{0.006}\text{Al}_{0.33}\text{Ti}_{0.12})(\text{Al}_{1.25}\text{Si}_{2.75})\text{O}_{10}$ $(\text{OH})_2 \cdot 0.05\text{Al}_6(\text{OH})_{15}$
	Stoichiometric difference between biotite and its weathering product reflecting conservation of the silicate sheet (coupling)	$\text{K}_{0.78}\text{Mg}_{0.34}\text{Ca}_{-0.017}\text{Na}_{-0.002}\text{Al}_{-0.30}\text{La}_{-0.000286}$

weathering rates (results not shown). This is due to the mass-balance calculations being dominated by a long-term data set (>20 years) of 6 major element flux values. For the mass-balance calculations used in this study, the plagioclase, and concomitantly allanite, dissolution rates are determined by the Na^+ flux, the biotite weathering rate is determined by the K^+ flux, the garnet dissolution rate is determined by the Ca^{2+} and/or Mg^{2+} fluxes, and the kaolinite and gibbsite weathering rates determined by the SiO_2 and Al^{3+} fluxes, respectively.

Major element proportions in biomass are treated here as stoichiometric proportions, in keeping with the “fictive-phase” approach formally expressed by Bowser and Jones (2002). In the absence of a widely accepted term for biomass as a fictive phases, the phrase “biomass stoichiometry” is used here in the interest of brevity because the fictive-phase concept allows such compositional proportions to be used in the same manner as stoichiometric coefficients. The same concept has been embraced by the Critical Zone and marine biologic communities using the phrases “biologic stoichiometry” and “elemental stoichiometry,” respectively (Quigg et al. 2003; Brantley et al. 2011). The weathering rates were also calculated using two different deciduous forest biomass macronutrient uptake stoichiometries. The first is from Velbel (1985a) and was determined from net primary production (NPP) values for CHL biomass published by Day and Monk (1977) and Boring et al. (1981). Velbel (1995) systematically investigated of the use of NPP-derived deciduous forest stoichiometries in Appalachian watershed mass-balance determinations of mineral weathering rates. The second deciduous forest biomass macronutrient uptake stoichiometry was calculated from seasonal changes in stream concentrations for a watershed developed on unreactive quartzite bedrock (Price et al. 2012). The quartzitic watershed is that of Bear Branch located in the northern Blue Ridge Physiographic Province, approximately 885 km northeast of CHL. Both CHL and the Bear Branch watershed have similar oak-hickory forest stands (Boring et al. 1981; Rice and Bricker 1995).

4 Results

4.1 Petrography

Fresh biotite at CHL is usually dark brown or green and strongly pleochroic in thin section. The first optical indication of biotite weathering is a change of pleochroism from green and strong to a weaker orange pleochroism, along and parallel to cleavage, and at biotite grain boundaries. At this stage of study, no preference of edge weathering over layer weathering, or vice versa, can be established. With increased weathering, cleavage traces are stained reddish brown, especially near grain boundaries. As weathering continues, lamellae of low pleochroism extend the entire length of the crystals, giving rise to interdigitation of high- and low-pleochroism lamellae. Weathered biotite with lowered pleochroism is usually pale yellow or orange in plane-polarized light. Occasionally, colorless first-order gray lamellae or lenses appear, as do lamellar or lenticular masses of reddish opaque material. Also, iron-stained “haloes” appear around some weathered biotites, suggesting that at least some of the iron in biotite is released and mobilized by weathering. The petrographic characteristics of biotite weathering at CHL are similar to those described elsewhere by numerous workers including Wilson (1966, 1970), Basham (1974), Bustin and Mathews (1979), Gilkes and Suddhiprakarn (1979a, b), Eswaren and Heng (1976), Meunier and Velde (1979a, b), Meunier (1980), and Bisdom et al. (1982).

4.2 Electron Microprobe Analyses (EMPA)

Individual electron microprobe analyses for both the biotite and its transformational weathering product are reported in Price et al. (2005a), with the compositions for each watershed reported in Table 2. The biotite weathering product for CHL has historically been referred to as vermiculite (e.g., Velbel 1985a; Price et al. 2005a). However, with a layer charge between 0.2 and 0.6, the biotite weathering products in Table 2 are technically smectite. Being hydroxy-interlayered, these smectites do not expand when magnesium-saturated samples are glycolated, thereby eliminating the widely used criteria for identifying smectite by XRD. The biotite weathering product reported in Table 2 reflects the composition of the most weathered trioctahedral mica from soil and is referred to herein as hydroxy-interlayered smectite (HIS). It is possible that early stage biotite weathering products may be vermiculitic with continued weathering resulting in the lower layer-charged smectite. In the absence of chemical analyses from which layer charge could be determined, the CHL biotite weathering product will be referred to as hydroxy-interlayered material (HIM).

The compositions of CHL biotite and its weathering product reported in Table 2 suggest that biotite weathering at CHL, as in most natural weathering environments, occurs by a “simple transformation” (Fanning and Keramidas 1977), in which the primary silicate structure is conserved. The composition of the biotite layer inferred from XRD and EPMA data is very similar to the biotite compositions analyzed by similar methods and reported from other watershed mass-balance studies on a variety of biotite-bearing parent rocks (e.g., O'Brien et al. 1997; Murphy et al. 1998).

4.3 X-Ray Diffraction

XRD patterns of clay-size fractions of regolith from several Coweeta watersheds (Fig. 2) show discrete 14 Å vermiculite or smectite peaks, 12 Å peaks, 10 Å mica peaks, 7.2 Å kaolin-group mineral peaks, and 4.85 Å gibbsite peaks. The 12 Å peak reflects a regularly interstratified 14 and 10 Å phase and may reflect either primary chlorite and biotite, and/or secondary vermiculite and biotite. In the case of the latter, similar d-spacings have been reported in soils of the southeastern USA as “mica-intermediate,” which may be hydroxy-interlayered hydrobiotite (Rebertus et al. 1986).

4.4 Scanning Electron Microscopy Secondary (SEM) and Backscattered Electron Imaging (BSE)

Weathering initially starts on the edges of the biotite (Fig. 3a, b) and is followed by weathering along cleavages planes that results in exfoliation (Fig. 3c). Parent biotite is gradually replaced by a transformational weathering produce of vermiculite and/or smectite (Fig. 3d). In the advanced stage of weathering, the transformational weathering product becomes replaced by neoformed kaolin-group minerals and/or gibbsite (Fig. 4a), although small quantities of the 2:1 phyllosilicate biotite weathering products remain (Fig. 4b). The features observed in Figs. 3 and 4 reflect dissolution of the 2:1 biotite sheets and replacement by kaolin-group minerals and/or gibbsite. Such textures provide evidence that the biotite silicate sheet is not entirely conserved during chemical weathering and that the assumption of a layer-for-layer stoichiometric relationship between biotite and its weathering product (e.g., Velbel 1985a; Taylor and Velbel 1991) is not justifiable. Therefore, decoupling biotite from its weathering product may be preferable in mass-balance calculations of mineral weathering rates (e.g., Cleaves et al. 1970; Price et al. 2005a).

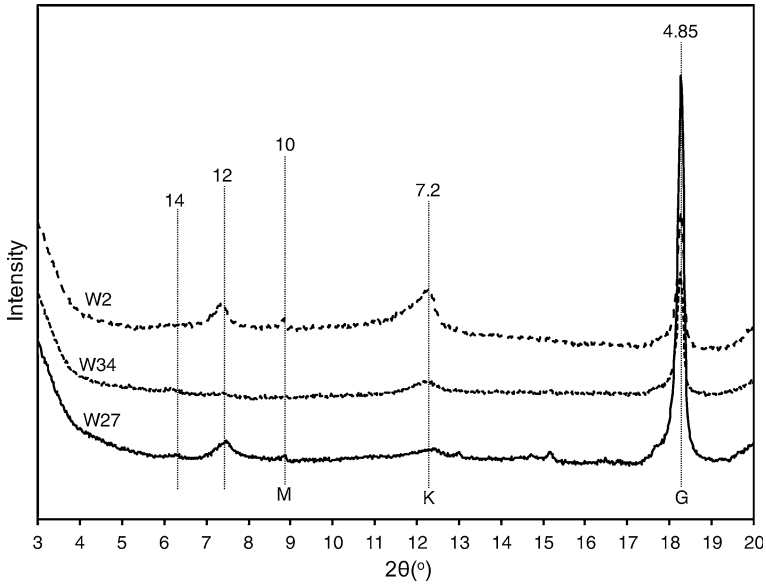
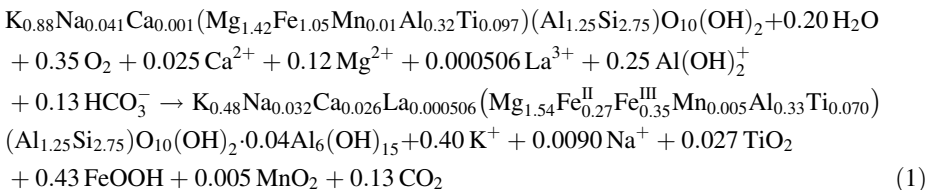


Fig. 2 Representative X-ray diffractograms for the watersheds investigated. Measurements above peaks are in Å. All samples are untreated and collected from the lower saprolite. The Watershed 34 sample is from Core 17 (Fig. 1). M = mica, K = kaolin-group, and G = gibbsite. The 12 and 14 Å peaks are not labeled as their specific mineralogy is not determined

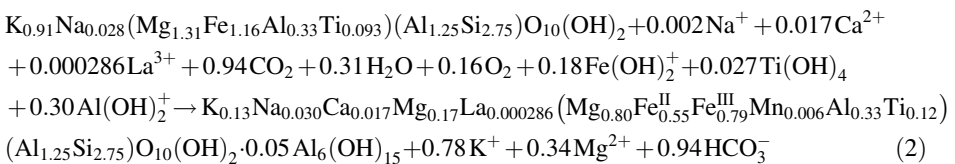
4.5 Biotite Weathering Reactions and Rates from Watershed Mass Balance

The rates of biotite weathering and formation of its weathering product determined from mass-balance methods are partly a function of whether reactant and product phyllosilicates are coupled or decoupled as defined above. Following Velbel (1985a, 1988), and Taylor and Velbel (1991), and using the compositions from Table 2, the coupled biotite weathering reactions for regolith developed on the Otto Formation and Coleman River Formation are written as follows:

Watersheds 2 and 34 (Otto Formation):



Watershed 27 (Coleman River Formation):



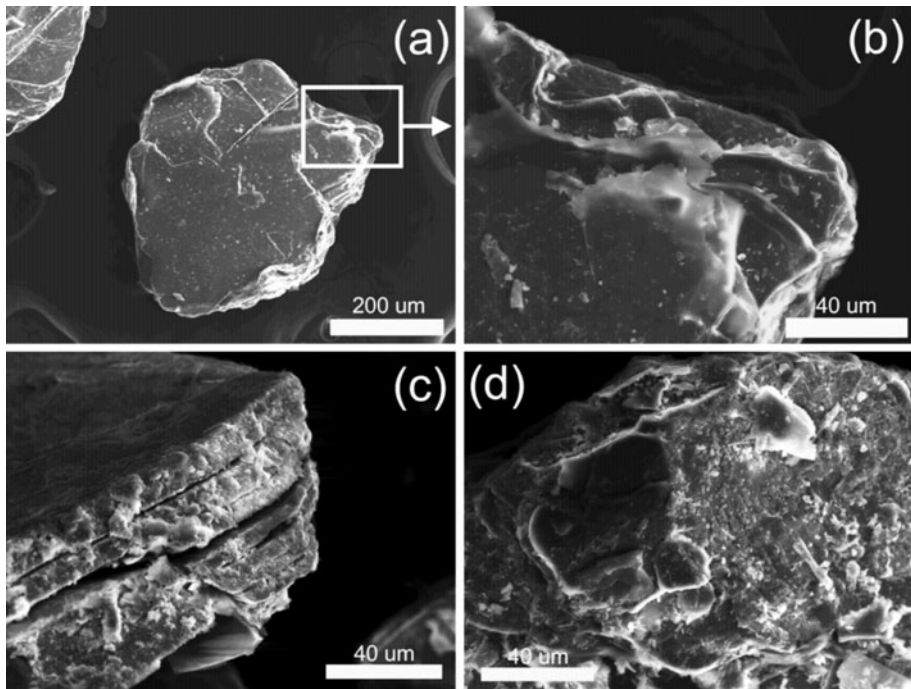
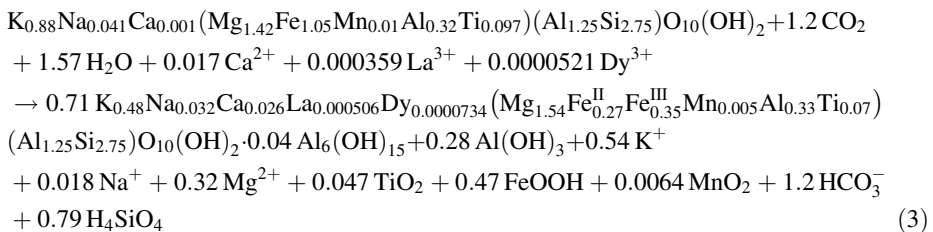


Fig. 3 SEM images of biotite in various stages of weathering. **a** Onset of weathering. **b** Inset of portion of biotite grain indicated in **a**. **c** Exfoliating weathering biotite. **d** Heavily weathered biotite with remnant of a biotite layer

The weathering rates of biotite and the formation rates of HIS for each watershed are provided in Table 3. Because they are coupled, their rates must be equal in magnitude, and opposite in sign as one is being consumed, while the other is produced.

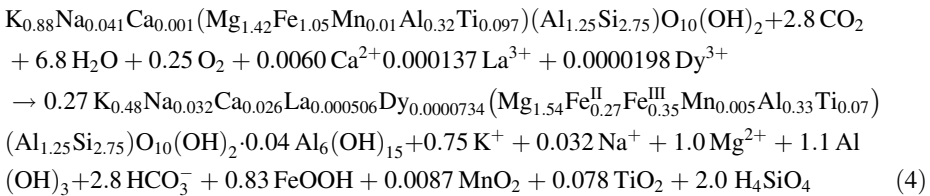
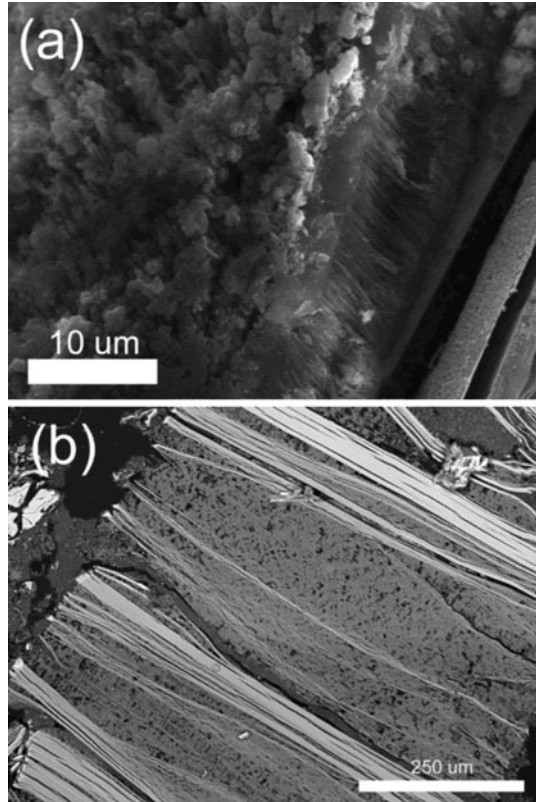
When biotite and its weathering product are decoupled, their stoichiometric relationship will be determined by their respective weathering rates (Table 3). Balanced weathering reactions for the decoupled scenario when the CHL NPP biomass stoichiometry is used are as follows:

Watershed 2 (Otto Formation):

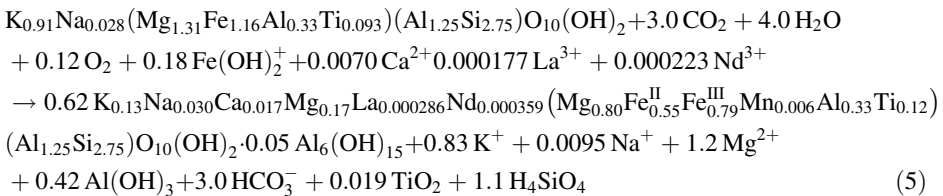


Watershed 34 (Otto Formation):

Fig. 4 Images of extensively weathered biotite grains. **a** SEM image of epitaxial neofomed secondary weathering products on heavily exfoliated biotite visible in the lower right. Sample from saprolite in Watershed 2. **b** BSE image of exfoliated weathering biotite with intercalated neofomed weathering products. Sample from A-horizon in Watershed 2



Watershed 27 (Coleman River Formation):



For the decoupled mass-balance results that used the Bear Branch biomass nutrient uptake stoichiometry, the stoichiometric relationship between biotite and HIS changes to 0.44, 0.11, and 0.56 vermiculite formula units per biotite formula unit for Watersheds 2, 34, and 27, respectively (Table 3).

Table 3 Results of the mass-balance calculations of mineral weathering rates for three control watersheds at Coweeta Hydrologic Laboratory, North Carolina, where positive value indicates destruction and a negative value indicates formation and all units of mol ha⁻¹ year⁻¹

Phase	Watershed 2			Watershed 34			Watershed 27					
	Coupled		Decoupled	Coupled		Decoupled	Coupled		Decoupled			
	CHL ^a	BB ^b										
Allanite	-776	-44	30	18	-673	-36	7	5	12	14	10	10
Plagioclase	774	515	485	483	688	463	435	442	242	242	243	240
Garnet	-5,813	-775	40	25	-4,869	-488	40	41	179	361	100	137
Biotite	-8,232	-526	433	305	-7,124	-422	142	127	154	228	112	124
HIS	8,232	526	-308	-134	7,124	422	-38	-14	-154	-228	-69	-69
Kaolin-group	9,532	1,171	-304	-320	8,091	819	-150	-166	-72	-348	-4	-78
Gibbsite	-8,763	-1,484	-288	-305	-7,612	-1,281	-513	-502	-486	-280	-546	-495
Biomass	3,367	284	-160	-130	2,928	247	-32	-26	-57	-115	-33	-41

^a Biomass macronutrient uptake stoichiometry of K_{1.0}Mg_{0.37}Ca_{0.96} from Velbel (1985a) and calculated from CHL forest net primary production values (Day and Monk 1977; Boring et al. 1981)

^b Biomass macronutrient uptake stoichiometry of K_{1.0}Mg_{1.1}Ca_{0.97} from Price et al. (2012) and calculated from the Bear Branch watershed underlain by quartzite

Regardless of whether the weathering reactions reflect coupling or decoupling, the initial compositional changes during weathering are due largely to removal of interlayer K^+ , as shown in reactions (1–5) above. There is also partial replacement of the released K^+ by gibbsite-like layers or aluminum-hydroxide “pillars.” Biotite weathering in all watersheds in all scenarios requires uptake of Ca^{2+} and La^{3+} by the HIS, with the Ca^{2+} being available from allanite, plagioclase, or garnet, and the La^{3+} being derived from the allanite (Price et al. 2005b). Plagioclase serves as the predominant source of Na^+ , a small amount of which is needed for the product in Watershed 27 as seen in the coupled scenario of reaction (2). Iron and Mg^{2+} may be derived from the weathering of garnet (Velbel 1985a; Velbel et al. 2009). Therefore, biotite weathering at CHL is capable of influencing the base cation concentrations of ambient soil and/or groundwater.

A significant difference in the results for the coupling and decoupling scenarios is that when biotite and HIS are coupled, there is only consumption of Al^{3+} , and no release of H_4SiO_4 as the silicate sheet is entirely conserved in the HIS. In contrast, when the biotite and HIS are decoupled, destruction of the silicate sheet yields both Al^{3+} and H_4SiO_4 . The Al^{3+} is then available for uptake during gibbsite precipitation, and both Al^{3+} and H_4SiO_4 are available for uptake during kaolin-group mineral precipitation. The HIS formation rate is lower than that of the biotite weathering rate regardless of biomass stoichiometry used (Table 3); this indicates that some of the silicate sheet of the biotite is being destroyed during weathering. Because the biotite is the only source for the Si^{4+} in tetrahedral sheets, it is not possible to have a HIS formation rate higher than that of the biotite weathering rate; that the calculations yield this geochemically reasonable outcome suggests there are no obvious or major flaws in the assumptions underlying the calculations.

For Watersheds 2 and 34, the mineral weathering rate results are geochemically unreasonable when the biotite and HIS rates are coupled (Table 3). This scenario yields calculated rates for allanite, garnet, and biotite weathering that are negative, indicating formation of these primary minerals during weathering, which is geochemically unreasonable. The formation of these phases at Earth's surface conditions is not thermodynamically and/or kinetically favorable, and these results may indicate that coupling biotite with its weathering product in geochemical-balance calculations of mineral weathering rates is not valid.

5 Discussion

With the exception of Watershed 2 which is known to have relatively high chemical weathering rates, the range of coupled biotite weathering rates reported in Table 3 are within the range of biotite weathering rates (36–200 mol ha^{-1} year $^{-1}$) calculated by O'Brien et al. (1997). O'Brien et al. (1997) did not incorporate biomass uptake of K^+ or Mg^{2+} into their mass balance. Taylor and Velbel (1991) showed that neglecting the biomass term in CHL watershed mass-balance calculations can cause mineral weathering rates to be underestimated by up to a factor of almost four relative to rates calculated to include biotic influence. The biotic effects were largest for biotite (Taylor and Velbel 1991), the weathering rate of which is calculated from the dissolved fluxes of K^+ , the most important plant nutrient among the major rock-forming elements. If the biotite weathering rates in the watersheds studied by O'Brien et al. (1997) are actually faster (by virtue of unaccounted for uptake of K^+ by biomass) than the rates calculated without considering biomass uptake of K^+ as published by O'Brien et al. (1997), then the range of biotite weathering rates calculated by O'Brien et al. (1997) may overlap the range calculated by Velbel (1985a),

Taylor and Velbel (1991), and Price et al. (2005a) (Table 3). Forest biomass within the Mid-Atlantic USA is known to be significantly aggrading and, therefore, capable of influencing calculated biotite weathering rates. When comparing different CHL watersheds on the same bedrock unit, the biotite weathering rate is found to be independent of stream discharge, at least over the range of discharges represented at CHL (Velbel 1985a).

Biotite weathering rates calculated for Coweeta watershed 27 in multiple mass-balance studies by Velbel (1985a; assuming a coupled biotite–vermiculite reaction), Taylor and Velbel (1991; assuming a coupled reaction, and invoking different long-term average solute fluxes), and Price et al. (2005a) and this study (assuming decoupled biotite-product reaction) were 187, 84, and 112 mol ha⁻¹ year⁻¹, respectively. When normalized to the estimated geometric surface area of biotite, the CHL biotite weathering rate from watershed 27 as calculated by Velbel (1985a) is 1.2×10^{-13} mol m⁻² s⁻¹ (log₁₀ rate = -12.9). The most recently mass-balance-determined biotite weathering rate for watershed 27, 112 mol ha⁻¹ year⁻¹ (Price et al. 2005a; Table 3) is 60 % of the corresponding rate estimated by Velbel (1985a); 60 % of Velbel's (1985a) surface-area-normalized rate is 7.2×10^{-14} mol m⁻² s⁻¹ (log₁₀ rate = -13.1). Although the three Coweeta watershed 27 biotite weathering rate estimates range over a factor of 2.2 (<0.4 log₁₀ units), any of these values is at the fast end of the range of natural surface-area-normalized biotite weathering rates compiled and tabulated by White (2002). The range of surface-area-normalized biotite weathering rates determined from natural systems (-13.0 > log₁₀ rate > -16.5; White 2002) are zero to six orders of magnitude slower than similarly normalized rates determined in laboratory experiments (including those of Acker and Bricker 1992, compiled and tabulated by White 2002). This difference between laboratory and field biotite weathering rates is identical in sign (field rates are slower) and similar in magnitude to the laboratory–field discrepancy long acknowledged and widely recognized in other rock-forming silicate-mineral groups (e.g., Velbel 1993; White and Brantley 2003).

As coupled reactions (1) and (2) are written, the formation rate of HIS layers equals the destruction rate of biotite layers (Table 3). Kaolin-group minerals and gibbsite are observed and form at CHL, but in the coupled scenario would have to form from Al³⁺ and Si⁴⁺ released by congruent dissolution of aluminosilicates other than micas (Velbel 1985a). In contrast, Price et al. (2005a) found that uncoupling all primary and secondary phases (including uncoupling HIS formation rate from biotite destruction rate) yields finite rates of HIS, kaolin-group minerals, and gibbsite production by weathering, all indicating that all are currently forming in the regolith at CHL. The HIS formation rate is lower than the biotite destruction rate in all watersheds investigated (Table 3), indicating that some HIS is being further weathered to kaolin-group minerals, and/or gibbsite, and solutes. Progressive destruction of earlier formed HIS to form kaolin-group minerals and/or gibbsite at CHL is consistent with the findings of Cleaves et al. (1970) at Pond Branch and elsewhere by O'Brien et al. (1997).

Coupling in mass-balance studies is justifiable if the structural and/or stoichiometric relationship between the parent biotite and its weathering product is known. In reactions (3–5) above and Table 3, the stoichiometric relationship between biotite and HIS are shown. If these stoichiometric relationships could be established prior to performing mass-balance calculations, then the number of unknowns would be reduced by one. For example, for the Loch Vale watershed, Colorado, Mast et al. (1990) and Mast (1992) invoked 0.87 mol of smectite–illite forming for every mole of biotite weathered.

The distribution and occurrence of weathering products is related to the reactivity of the bedrock and rapidity of water movement through the watersheds (Velbel 1985b). With the metagraywacke Otto Formation being mineralogically immature relative to the

metasandstone Coweeta Group, the formation rates of the secondary weathering products may be investigated as a function of bedrock reactivity. Similarly, a large precipitation gradient occurs across CHL, with relatively high precipitation occurring in the western portion of the basin (Table 1; Fig. 1). Watershed 2 represents relatively low flushing of relatively high reactivity silica-releasing bedrock (Table 1; Fig. 5) and is characterized by the highest kaolin-group mineral formation rates and lowest gibbsite formation rates. Watershed 27 represents the opposite extremum, with relatively high flushing, relatively low rock reactivity, and the lowest SiO₂ flux of the three watersheds investigated (Table 1). This watershed is characterized by the lowest kaolin-group formation rates and high gibbsite formation rates (Fig. 5). Watershed 34 is intermediate, with relatively high flushing of relatively high reactivity bedrock, and the highest SiO₂ flux of the three watersheds investigated (Table 1). The kaolin-group formation rate for Watershed 34 is intermediate between that of Watersheds 2 and 27, but Watershed 34 still exhibits a gibbsite formation rate comparable to that of Watershed 27 (Fig. 5). This is consistent with the clay mineral distributions among Coweeta watersheds reported by Velbel (1984b), and their relation to the solute abundances and mineral-solution thermodynamic relations reported by Velbel (1985b). High flushing rates result in rapid silica removal, limiting kaolin-group mineral production and retaining most Al³⁺ released by aluminosilicate weathering in gibbsite. Low flushing rates result in slower silica removal, more Al³⁺ released by aluminosilicate weathering reactions is retained in kaolin-group minerals, and less Al³⁺ remains uncombined with silica as gibbsite. The more reactive rock types undergo more aluminosilicate weathering for a given flushing rate than the less reactive rock types, releasing more silica into the same amount of solution and thereby favoring kaolin-group mineral production over gibbsite. Solute concentrations and degree of evolution of solution compositions toward thermodynamic mineral-solution equilibrium show the same relationships (Velbel 1985b).

The diffractograms in Fig. 2 reflect clay mineral formation occurring integrated over geologic timescales (Price et al. 2005a), and the stream water solute chemistry reflects geochemical processes operating for the multi-decadal period of sampling (Velbel 1985b). The comparability between the clay minerals identified in the diffractograms and the calculated mineral weathering rates may be interpreted to indicate that the relative environmental differences (environmental gradients) between the three watersheds investigated are invariant over geologic time.

	High Discharge (Flushing Rate) (35-51 m ³ ha ⁻¹ day ⁻¹)	Low Discharge (Flushing Rate) (25 m ³ ha ⁻¹ day ⁻¹)
High Bedrock Reactivity (Otto Formation)	<u>Watershed 34</u> Kaolin-group = 150 to 166 mol ha ⁻¹ yr ⁻¹ Gibbsite = 502 to 513 mol ha ⁻¹ yr ⁻¹	<u>Watershed 2</u> Kaolin-group = 304 to 320 mol ha ⁻¹ yr ⁻¹ Gibbsite = 288 to 305 mol ha ⁻¹ yr ⁻¹
Low Bedrock Reactivity (Coweeta Group)	<u>Watershed 27</u> Kaolin-group = 4 to 78 mol ha ⁻¹ yr ⁻¹ Gibbsite = 495 to 546 mol ha ⁻¹ yr ⁻¹	No data available

Fig. 5 Matrix showing the influence of bedrock reactivity and discharge (flushing rate) on clay mineral neof ormation rates. All rates reflect decoupling of biotite from its weathering product with the range reflecting the different biomass stoichiometries used

Not surprisingly, the effects of the chosen biomass stoichiometry on calculated biotite and HIS weathering rates are most significant for Watershed 2 which exhibits the highest rate of biomass nutrient uptake (Table 3). The differences in the biotite weathering rate for Watershed 2 for the two biomass stoichiometries investigated is 30 %. For the other two watersheds, this difference does not exceed 11 %. However, the difference in the HIS formation rate can be dramatic depending on the biomass stoichiometry used, with differences of 56 and 63 % for Watershed 2 and Watershed 34, respectively. Additional work is needed in the determination of an appropriate biomass nutrient uptake stoichiometry for application to watershed mass-balance studies.

6 Conclusions

The watershed mass-balance-calculated weathering rates of biotite and its transformational weathering product have been investigated for Coweeta Hydrological Laboratory. These values may vary dramatically depending on (1) whether the biotite rate is stoichiometrically coupled to its transformational weathering product and (2) the biomass stoichiometry used. The findings of this study are consistent with transmission electron microscopic observations that show the biotite silicate sheet dissolving and yielding Al^{3+} and Si^{4+} available for uptake during precipitation of neoformed clays. Coupling of biotite and its transformational weathering product is valid only if the structural and/or stoichiometric relationship of the two phases is explicitly known.

Rates of biotite weathering and transformation of its secondary weathering product at CHL are comparable with other Appalachian mass-balance studies in which the destruction and production reactions of these two minerals are decoupled. When normalized to the estimated surface area, the biotite weathering rates calculated for CHL are lower than those measured in the laboratory. The magnitude of this laboratory–field discrepancy is similar to that for other primary silicate minerals. The influence of biomass stoichiometry on the rates of biotite weathering and transformational weathering product is highest for watersheds with high biomass aggradation rates.

The distribution and occurrence of neoformed kaolin-group minerals and gibbsite is a function of bedrock reactivity and the rapidity of water movement through the watersheds. Relatively high bedrock reactivity and relatively high rates of water movement yield intermediate rates of formation of both kaolin-group minerals and gibbsite. The opposite scenario of relatively low bedrock reactivity and relatively low rates of water movement yield relatively low rates of kaolin-group mineral formation and relatively high rates of gibbsite formation. A watershed developed on relatively high bedrock reactivity and relatively high rates of water movement yields intermediate kaolin-group mineral formation rates, but relatively high gibbsites formation rates. The similarity between the calculated rates and relative abundances determined from X-ray diffractograms indicates that the relative environmental differences between the watersheds investigated are invariant on geologic timescales.

Acknowledgments The second author is grateful to Robert A. Berner, Brij L. Sawhney, Robert J. Tracy, Garth K. Voigt, and the late Finley C. Bishop, for introducing him to mica crystal chemistry, clay mineralogy and weathering. After the second author relocated to Michigan State University (MSU), Max M. Mortland generously shared his experience and insights into mica weathering, for which the second author is most grateful. An early version of this work was presented at the 1985 annual meeting of the Soil Science Society of America; Joe Dixon is thanked for his comments on that presentation. Several former MSU graduate students (in addition to the first author) have contributed to the second author's understanding of

biotite weathering at CHL, especially Allan B. Taylor and Daniel Gierman. The second author is also indebted to Warren Huff for his helpful advice, and Emery T. Cleaves, Karl K. Turekian, Blair F. Jones and Owen P. Bricker for their encouragement. Early biotite weathering studies at CHL were supported by NSF Grant EAR 80-07815 (R.A. Berner, P.I.). Continued mass-balance studies of silicate-mineral weathering at CHL by the first author were supported by a Grant-in-Aid of Research and Sigma Xi. Additional funding was provided by a Michigan Space Grant Consortium Graduate Fellowship, Clay Minerals Society Student Grant, and a Lucile Drake Pringle Fellowship. The authors thank two anonymous reviewers whose thoughtful reviews greatly improved this manuscript and Suzanne Bricker for editorial handling.

References

- Acker JG, Bricker OP (1992) The influence of pH on biotite dissolution and alteration kinetics at low temperature. *Geochim Cosmochim Acta* 56:3073–3092
- Aubert D, Stille P, Probst A (2001) REE fractionation during granite weathering and removal by waters and suspended loads: Sr and Nd isotopic evidence. *Geochim Cosmochim Acta* 65:387–406
- Banfield JF, Eggleton RA (1988) A transmission electron microscope study of biotite weathering. *Clays Clay Miner* 36:47–60
- Basham IR (1974) Mineralogical changes associated with deep weathering of gabbro in Aberdeenshire. *Clay Miner* 10:189–202
- Berner RA, Berner EK (1997) Silicate weathering and climate. In: Ruddiman WF (ed) *Tectonic uplift and climate change*. Plenum Press, New York, pp 353–365
- Berry JL (1976) Study of chemical weathering in the Coweeta Hydrologic Laboratory, Macon County, NC. Unpublished report
- Bisdorn EBA, Stoops G, Delvigne J, Curmi P, Altemüller HJ (1982) Micromorphology of weathering biotite and its secondary products. *Pedologie* 32:225–252
- Boring LR, Monk CD, Swank WT (1981) Early regeneration of a clear-cut southern Appalachian forest. *Ecology* 62:1244–1253
- Bowser CJ, Jones BF (2002) Mineralogical controls on the composition of natural waters dominated by silicate hydrolysis. *Am J Sci* 32:582–662
- Brantley SL, Megoñal JP, Scatena FN, Balogh-Brunstad Z, Barnes RT, Bruns MA, van Cappellen P, Dontsova K, Hartnett HE, Hartshorn AS, Heimsath A, Herndon E, Jin L, Keller CK, Leake JR, McDowell WH, Meinzer FC, Mozdzer TJ, Petsch S, Pett-Ridge J, Pregitzer KS, Raymond PA, Riebe CS, Shumaker K, Sutton-Grier A, Walter R, Yoo K (2011) Twelve testable hypotheses on the geobiology of weathering. *Geobiology* 9:140–165
- Bricker OP, Godfrey AE, Cleaves ET (1968) Mineral-water interaction during the chemical weathering of silicates. In: Gould RF (ed) *Trace inorganics in water*. Advances in Chemistry Series 73, American Chemical Society, Washington, DC, pp 128–142
- Bricker OP, Jones BF, Bowser CJ (2003) Mass-balance approach to interpreting weathering reactions in watershed systems. In: Holland HD, Turekian KK (ex eds), Drever JI (ed) *Treatise on geochemistry*, vol. 5, Surface and ground water, weathering, and soils. Elsevier, New York, pp 119–132
- Brown G, Brindley GW (1984) X-ray diffraction procedures for clay mineral identification. In: Brindley GW, Brown G (eds) *Crystal structures of clay minerals and their x-ray identification*. Mineralogical Society of London, London, pp 305–360
- Bustin EM, Mathews WH (1979) Selective weathering of granitic clasts. *Can J Earth Sci* 16:215–223
- Ciamponi MA (1995) Non-systematic weathering profile on metamorphic rock in the southern Blue Ridge Mountains, North Carolina: petrography, bulk chemistry, and mineral chemistry of biotite. Thesis, University of Cincinnati
- Cleaves ET, Godfrey AE, Bricker OP (1970) Geochemical balance of a small watershed and its geomorphic implications. *Geol Soc Am Bull* 81:3015–3032
- Creasey J, Edwards AC, Reid JM, MacLoud DA, Cresser MS (1986) The use of catchment studies for assessing chemical weathering rates in two contrasting upland areas in northeast Scotland. In: Colman SM, Dethier DP (eds) *Rates of chemical weathering of rocks and minerals*. Academic Press, New York, pp 467–502
- Day FP, Monk CD (1977) Seasonal nutrient dynamics in the vegetation on a southern Appalachian watershed. *Am J Bot* 64:1126–1139
- Deer WA, Howie RA, Zussman J (1966) *An introduction to the rock-forming minerals*. Longmans, London
- Dessert C, Dupré B, Gaillardet J, François LM, Allègre CJ (2003) Basalt weathering laws and the impact of basalt weathering on the global carbon cycle. *Chem Geol* 202:257–273

- Dong H, Peacor DR, Murphy SF (1998) TEM study of progressive alteration of igneous biotite to kaolinite throughout a weathered soil profile. *Geochim Cosmochim Acta* 62:1881–1887
- Drever JI (1973) The preparation of oriented clay mineral specimens for X-ray diffraction analysis by a filter-membrane peel technique. *Am Min* 58:553–554
- Eslinger E, Pevear D (1988) Clay minerals for petroleum geologists and engineers. Society of Economic Geologists and Paleontologists Short Course Notes 22
- Eswaren H, Heng YY (1976) The weathering of biotite in a profile on gneiss in Malaysia. *Geoderma* 16:9–20
- Fanning DS, Keramidas VZ (1977) Micas. In: Dixon JB, Weed SB (eds) *Minerals in soil environments*. Soil Science Society of America, Madison, pp 195–258
- Gaillardet J, Dupré B, Louvat P, Allègre CJ (1999) Global silicate weathering and CO₂ consumption rates deduced from the chemistry of large rivers. *Chem Geol* 159:3–30
- Gammons CH, Wood SA, Nimick DA (2005) Diel behavior of rare earth elements in a mountain stream with acidic to neutral pH. *Geochim Cosmochim Acta* 69:3747–3758
- Garrels RM, Mackenzie FT (1967) Origin of the chemical compositions of some springs and lakes. In: Stumm W (ed) *Equilibrium concepts in natural water systems*. American Chemical Society Advances in Chemistry Series 67, Washington, DC, pp 222–242
- Gilkes RJ, Suddhiprakarn A (1979a) Biotite alteration in deeply weathered granite. I. Morphological, mineralogical, and chemical properties. *Clays Clay Miner* 27:349–360
- Gilkes RJ, Suddhiprakarn A (1979b) Biotite alteration in deeply weathered granite. II. The oriented growth of secondary minerals. *Clays Clay Miner* 27:361–367
- Gilkes RJ, Young RC, Quirk JP (1972) The oxidation of octahedral iron in biotite. *Clays Clay Miner* 20:303–315
- Hatcher RD (1980) Geologic map of Coweeta Hydrologic Laboratory, Prentiss Quadrangle, North Carolina. State of North Carolina, Department of Natural Resources and Community Development, in Cooperation with the Tennessee Valley Authority, scale 1:14,400
- Hatcher RD (1988) Bedrock geology and regional geologic setting of Coweeta Hydrologic Laboratory in the Eastern Blue Ridge. In: Swank WT, Crossley DA Jr (eds) *Forest hydrology and ecology at Coweeta*. Springer, New York, pp 81–92
- Hewlett JD (1961) Soil moisture as a source of base flow from steep mountain watersheds. Southeastern Forest Experiment Station Paper 132, U.S. Department of Agriculture-Forest Service, Asheville, NC
- Hewlett JD, Hibbert AR (1963) Moisture and energy conditions within a sloping soil mass during drainage. *J Geophys Res* 68:1081–1087
- Hughes RE, Moore DM, Glass HD (1994) Qualitative and quantitative analysis of clay minerals in soils. In: Amonette JE, Zelazny LW (eds) *Quantitative methods in soil mineralogy*. Soil Science Society of America Miscellaneous Publications, Madison, pp 330–359
- Ingri J, Widerlund A, Land M, Gustafsson Ö, Andersson P, Öhlander B (2000) Temporal variations in the fractionation of the rare earth elements in a boreal river; the role of colloidal particles. *Chem Geol* 166:23–45
- Likens GE, Bormann FB (1995) *Biogeochemistry of a forested ecosystem*. Springer, New York
- Mast MA (1992) Geochemical characteristics. In: Baron J (ed) *Biogeochemistry of a subalpine ecosystem: Loch Vale watershed*. Springer Ecological Studies Series No 90. Springer, New York, pp 93–107
- Mast MA, Drever JI, Baron J (1990) Chemical weathering in the Loch Vale watershed, Rocky Mountain National Park, Colorado. *Water Resour Res* 26:2971–2978
- Meunier A (1980) Les mécanismes de l'altération des granites et le rôle des microsystèmes. Etude des arènes du massif granitique de Parthenay (Deux-Sèvres). *Mém Soc Géol Fr LIX*
- Meunier A, Velde B (1979a) Biotite weathering in granites of western France. In: Mortland MM, Farmer VC (eds) *Proceedings of the international clay conference 1978*. Elsevier, New York, pp 405–413
- Meunier A, Velde B (1979b) Weathering mineral facies in altered granites: the importance of local small-scale equilibria. *Miner Mag* 43:261–268
- Miller CF, Hatcher RD Jr, Ayers JC, Coath CD, Harrison TM (2000) Age and zircon inheritance of eastern Blue Ridge plutons, southwestern North Carolina and northeastern Georgia, with implications for magma history and evolution of the southern Appalachian orogen. *Am J Sci* 300:142–172
- Moore DM, Reynolds RC Jr (1997) *X-ray diffraction and the identification and analysis of clay minerals*. Oxford University Press, New York
- Murphy SF, Brantley SL, Blum AE, White AF, Dong H (1998) Chemical weathering in a tropical watershed, Luquillo Mountains, Puerto Rico: II. Rate and mechanism of biotite weathering. *Geochim Cosmochim Acta* 62:227–243
- Newman ACD (1987) *Chemistry of clays and clay minerals*. Wiley, New York
- Newman ACD, Brown G (1966) Chemical changes during the alteration of micas. *Clay Miner* 6:297–310

- Norrish K (1973) Factors in the weathering of mica to vermiculite. In: Proceedings of the international clay conference 1972, pp 417–432
- O'Brien AK, Rice KC, Bricker OP, Kennedy MM, Anderson RT (1997) Use of geochemical mass balance modelling to evaluate the role of weathering in determining stream chemistry in five Mid-Atlantic watersheds of different lithologies. *Hydrol Process* 11:719–744
- Oliva P, Viers J, Dupré B (2003) Chemical weathering in granitic environments. *Chem Geol* 202:225–256
- Plummer LN, Back W (1980) The mass-balance approach: application to interpreting the chemical evolution of hydrologic systems. *Am J Sci* 280:130–142
- Price JR, Velbel MA, Patino LC (2005a) Rates and timescales of clay-mineral formation by weathering in saprolitic regoliths of southern Appalachian Mountains from geochemical mass balance. *Geol Soc Am Bull* 117:783–794
- Price JR, Velbel MA, Patino LC (2005b) Allanite and epidote weathering at the Coweeta Hydrologic Laboratory, western North Carolina, USA. *Am Miner* 90:101–114
- Price JR, Rice K, Szymanski D (2012) Mass-balance modeling of mineral weathering rates and CO₂ consumption in the forested Hauer Branch watershed, Catoctin Mountain, Maryland, USA. *Earth Surf Proc Land*. doi:10.1002/esp.3373
- Puckett LJ, Bricker OP (1992) Factors controlling the major ion chemistry of streams in the Blue Ridge and Valley and Ridge physiographic provinces of Virginia and Maryland. *Hydrol Process* 6:79–98
- Quigg A, Finkel ZV, Irwin AJ, Rosenthal Y, Ho TY, Reinfelder JR, Schofield O, Morel FMM, Falkowski PG (2003) The evolutionary inheritance of elemental stoichiometry in marine phytoplankton. *Nature* 425:291–294
- Rebertus RA, Weed SB, Buol SW (1986) Transformations of biotite to kaolinite during saprolite-soil weathering. *Soil Sci Soc Am J* 50:810–819
- Rice KC, Bricker OP (1995) Seasonal cycles of dissolved constituents in streamwater in two forested catchments in the mid-Atlantic region of the eastern USA. *J Hydrol* 170:137–158
- Schroeder PA, Melear ND, West LT, Hamilton DA (2000) Meta-gabbro weathering in the Georgia Piedmont, USA: implications for global silicate weathering rates. *Chem Geol* 163:235–245
- Smith JT, Fesenko SV, Howard BJ, Horrill AD, Sanzharova NI, Alexakhim RM, Elder DG, Naylor C (1999) Temporal change in fallout ¹³⁷Cs in terrestrial and aquatic systems: a whole ecosystem approach. *Environ Sci Technol* 33:49–54
- Stallard RF, Edmond JM (1983) Geochemistry of the Amazon 2. The influence of geology and weathering environment on the dissolved load. *J Geophys Res* 88:9671–9688
- Swank WT, Crossley DA Jr (1988) Introduction and Site Description. In: Swank WT, Crossley DA Jr (eds) *Forest hydrology and ecology at Coweeta*. Springer, New York, pp 3–16
- Swank WT, Waide JB (1988) Characterization of baseline precipitation and stream chemistry and nutrient budgets for control watersheds. In: Swank WT, Crossley DA Jr (eds) *Forest hydrology and ecology at Coweeta*. Springer, New York, pp 57–79
- Swift LW Jr, Cunningham GB, Douglass JE (1988) Climatology and hydrology. In: Swank WT, Crossley DA Jr (eds) *Forest hydrology and ecology at Coweeta*. Springer, New York, pp 35–56
- Taylor AB, Velbel MA (1991) Geochemical mass balance and weathering rates in forested watersheds of the southern Blue Ridge. II. Effects of botanical uptake terms. *Geoderma* 51:29–50
- Thomson ML, Ukrainczyk L (2002) Micas. In: Dixon JB, Schulze DG (eds) *Soil mineralogy with environmental applications*. Soil Science Society of America, Madison, pp 431–466
- Velbel MA (1984a) Weathering processes of rock-forming minerals. In: Fleet ME (ed) *Environmental geochemistry*. Mineralogical Association of Canada Short Course Handbook 10, pp 67–111
- Velbel MA (1984b) Mineral transformations during rock weathering, and geochemical mass-balances in forested watersheds of the southern Appalachians. Yale University, Dissertation
- Velbel MA (1985a) Geochemical mass balances and weathering rates in forested watersheds of the southern Blue Ridge. *Am J Sci* 285:904–930
- Velbel MA (1985b) Hydrogeochemical constraints on mass balances in forested watersheds of the southern Appalachians. In: Drever JI (ed) *The chemistry of weathering*. Reidel, Dordrecht, pp 231–247
- Velbel MA (1986) The mathematical basis for determining rates of geochemical and geomorphic processes in small forested watersheds by mass balance: Examples and implications. In: Colman SM, Dethier DP (eds) *Rates of chemical weathering of rocks and minerals*. Academic Press, Orlando, pp 439–451
- Velbel MA (1988) Weathering and soil-forming processes. In: Swank WT, Crossley DA Jr (eds) *Forest hydrology and ecology at Coweeta*. Springer, New York, pp 93–102
- Velbel MA (1993) Constancy of silicate-mineral weathering-rate ratios between natural and experimental weathering: implications for hydrologic control of differences in absolute rates. *Chem Geol* 105:89–99
- Velbel MA (1995) Interaction of ecosystem processes and weathering. In: Trudgill S (ed) *Solute modelling in catchment systems*. Wiley, New York, pp 193–209

- Velbel MA, Price JR (2007) Solute geochemical mass-balances and mineral weathering rates in small watersheds: methodology, recent advances, and future directions. *Appl Geochem* 22:1682–1700
- Velbel MA, Donatelle AR, Formolo MJ (2009) Reactant-product textures, volume relations, and implications for major-element mobility during natural weathering of hornblende, Tallulah Falls Formation, Georgia Blue Ridge, U.S.A. *Am J Sci* 309:661–688
- White AF (2002) Determining mineral weathering rates based on solid and solute weathering gradients and velocities: application to biotite weathering in saprolites. *Chem Geol* 190:69–89
- White AF (2003) Natural weathering rates of silicate minerals. In: Holland HD, Turekian KK (ex eds), Drever, JI (ed) *Treatise on geochemistry*, vol. 5, Surface and ground water, weathering, and soils. Elsevier, New York, pp 133–168
- White AF, Brantley SL (2003) The effect of time on the weathering of silicate minerals: why do weathering rates differ in the laboratory and field? *Chem Geol* 202:479–506
- Wilson MJ (1966) The weathering of biotite in some Aberdeenshire soils. *Miner Mag* 35:1080–1093
- Wilson M (1970) A study of weathering in a soil derived from a biotite-hornblende rock. I. Weathering of biotite. *Clay Miner* 8:291–303
- Wilson MJ (1987) X-ray powder diffraction and methods. In: Wilson MJ (ed) *A handbook of determinative methods in clay mineralogy*. Chapman and Hall, New York, pp 26–98
- Yeakley JA, Swank WT, Swift LW, Hornberger GM, Shugart HH (1998) Soil moisture gradients and controls on a southern Appalachian hillslope from drought through recharge. *Hydrol Earth Syst Sci* 2:41–49